



TD-DFT insights into the sensing potential of the luminescent covalent organic framework for indoor pollutant formaldehyde

Manzoor Hussain ^{a, b}, Xuedan Song ^{a, *}, Shaheen Shah ^b, Ce Hao ^a

^a State Key Laboratory of Fine Chemicals, Dalian University of Technology, Dalian 116024, China

^b Department of Chemistry, Karakoram International University (KIU), Gilgit 15100, Gilgit-Baltistan, Pakistan

ARTICLE INFO

Article history:

Received 21 January 2019

Received in revised form 26 July 2019

Accepted 26 July 2019

Available online 27 July 2019

Keywords:

Luminescent (TT-COF)

Electronically excited states

Hydrogen bonding

MOMAP

ABSTRACT

This paper investigates the sensitivity of the luminescent thieno[2,3-*b*]thiophene-based covalent organic framework (TT-COF) towards the formaldehyde using the density functional theory and time-dependent method. The hydrogen bonding dynamics is explored by comparison of geometries, electronic transition energies, binding energies, UV–vis, and infrared spectra. Frontier molecular orbitals examination, natural population analysis, and plotted electron density difference map describe the quenching process explicitly via electron density distribution. The MOMAP program illuminates the quenching owing to TT-COF-HCHO complex radiative rate constant. Furthermore, the S1-T1 energy gap describes the facilitation of the luminescence quenching through the intersystem crossing. Above all results elaborate the TT-COF's potential to detect the formaldehyde.

© 2019 Elsevier B.V. All rights reserved.

1. Introduction

Intermolecular hydrogen bonding results from the specific interaction between a hydrogen atom of a molecule or a molecular fragment with a highly electronegative atom or group of atoms from another molecule [1,2]. These relatively robust types of dipole-dipole forces are as the site-specific interactions of a hydrogen donor and acceptor molecules in gaseous or solution phase [3–5]. The phenomenon of hydrogen bonding plays a pivotal role, having significant impacts on the photophysics and photochemistry of chromophores. Thus, it provides a major insight into the in-depth understanding of the microscopic structure and function of various molecular systems [6]. Therefore scientists have been widely acknowledged its importance in chemistry, physics, biology, material sciences, and chemical physics disciplines and inter-disciplines. Moreover, theoretical and experimental investigations have extensively been made regarding the nature of hydrogen bonding in biological and organic molecules for electronic excitation states. Amongst those devoted endeavors, the Zhao and Liu work is considered as a significant breakthrough, mainly, the hydrogen bonding dynamics and influence on deactivation process [7]. The theoretical and experimental study by Han et al. validated the facilitation of nonadiabatic processes, i.e., internal conversion (IC), intersystem crossing (ISC), photoinduced electron transfer (PET), twisted intramolecular charge transfer, site-specific solvation via electronically excited intermolecular hydrogen bonding dynamics

[8–10]. Hao et al. have theoretically investigated the hydrogen bonding interactions for many systems, e.g., metal-organic frameworks, organic supramolecular systems, and COFs with various solvents, analytes, pollutants, nitroaromatics and other aromatic explosives in the electronic excited state [11–13].

Thus, the comprehensions of hydrogen bonds' dynamics can be expended for the luminescent COFs with the promising availability of functionals having the potential to act as photochemical sensors. Based on, COFs extra stability, high porosity, low-density, and high conjugation architecture together endow them with noteworthy applications, i.e., in gas storage, chemo-sensing and separation [14–16]. For the investigation of noncovalent interactions, the more straightforward and robust tools like DFT and TD-DFT quantum-chemical methods can successfully be employed [17]. Thereby, the current research of hydrogen bonding between COF and organic pollutant has accomplished via DFT and TD-DFT approaches. In this context, we first time utilized the TT-COF synthesized by Knochel et al. through the co-condensation of thieno[3,2-*b*]thiophene-2,5-diylidiboronic acid (TTBA) and the polyol 2,3,6,7,10,11-hexahydroxytriphenylene (HHTP) to get insights into the electronically excited state hydrogen bonds' nature. Luckily, TT-COF displays the periodic pattern, high surface area, well organized porous crystallinity, robust thermal stability, and boronate ester functionality; endow with high charge-carrier mobilities as well as the significant photoresponsive character [18].

Similarly, the selected formaldehyde analyte is known as the primary indoor pollutant and quite hazardous for human eyes and respiratory system. Owing to its high concentrations and upon prolonged exposure can lead to leukemia. Also, the formaldehyde is

* Corresponding author.

E-mail address: song@dlut.edu.cn (X. Song).

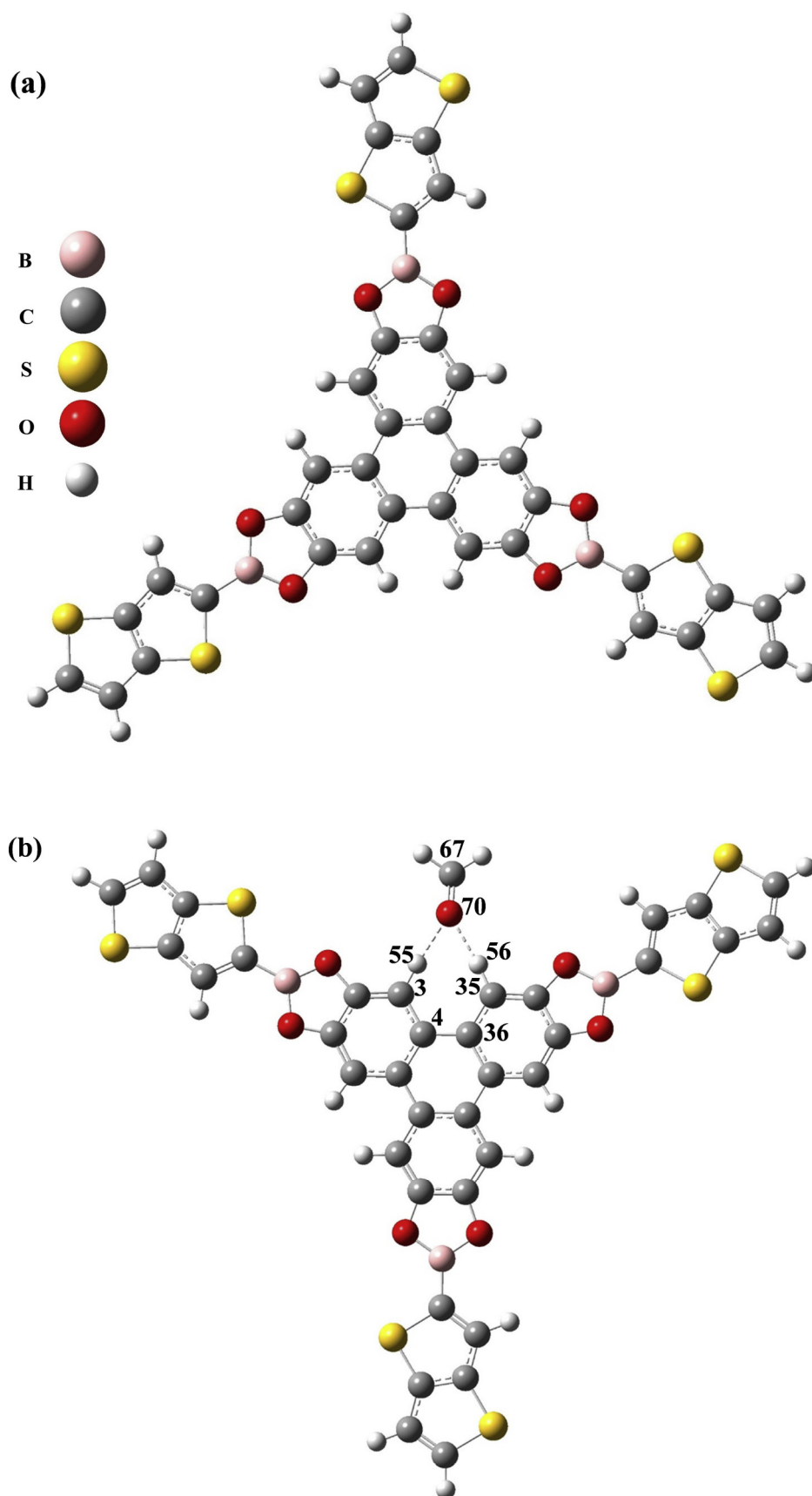


Fig. 1. Optimized structures. (a) Representative TT-COF fragment. (b) TT-COF-HCHO complex.

the level 1 carcinogen, causes nasopharyngeal carcinoma [19–21]. Additionally, according to the formaldehyde structure, the electronegative oxygen atom of carbonyl functional contains two free lone pairs of electrons can behave as hydrogen acceptor with hydrogen donor luminescent chromophore due to the presence boronic ester group to the aromatic system of HHTP skeleton. Hence, we assume that photoexcited hydrogen bonding can bring new understandings of the TT-COF sensitivity.

2. The computational details

2.1. Computational model

For all theoretical computations, the selected truncated fragment represents the entire TT-COF system shown in Fig. 1a. This star type fragment is containing three thieno[3,2-*b*]thiophene moieties linked to the triphenylene unit directly via a boronic ester linkage to form the 2D periodic layers. Then, to get the saturation on truncated terminals, added hydrogen atoms are presented in Fig. 1a. Similarly, the formaldehyde was introduced to investigate the hydrogen bonding and the resulting influence on the luminescent behavior. Amongst various optimized hydrogen-bonded complexes, the most stable isomer with minimum energy was designated for further calculations. In Fig. 1b the hydrogen bonded dimer adequately denotes its atomic locations.

2.2. Computational methods

The Gaussian 09 program suit was employed to perform the electronic geometry calculation [22]. Where the S0 optimization, IR frequencies, and NBO analysis were carried out using B3LYP in combination with 6-31G+(d) basis set [23]. However, the TD-DFT at B3LYP/6-31G+(d) level was used to estimate the UV–vis, electronic transition, excitation state optimization, and other S1 state computations. Moreover, by the ADF 2012 program, we calculated the electronic configurations with the B3LYP hybrid functional and TZP basis set [24,25]. Similarly, the binding energy was determined from the counterpoise method, as follows [26]:

$$E_{\text{binding}} = E_{\text{TT-COF-HCHO complex}} - E_{\text{TT-COF}} - E_{\text{HCHO}} + E_{\text{BSSE}}$$

Additionally, the electron density difference map was plotted by the multifunctional program, the Multiwfn [27]. To gain insights into the quenching trend used the TD-DFT method for T1 optimization and determined the S1-T1 energy gap difference [28]. By MOMAP program developed by Shuai's research group estimated the fluorescence rate constant [29].

3. Results and discussion

3.1. Structure optimization

According to the provided results in Table 1, the computed geometry parameters including required bond lengths, bond angles, vibration frequencies, and emission spectrum are entirely compatible with the corresponding crystal structure of the selected TT-COF [18]. The computed UV–Vis absorption 347 nm, as seen the black line spectrum in Fig. 2 compared to the experimental spectrum (red line) of 360 nm value. Therefore it can conclude that the B3LYP/6-31G+(d) approach is a better choice for the investigation of hydrogen bonding. This consistency in results further confirms the viability of a truncated fragment as representative of the whole periodic framework.

Table 1

Comparison of theoretical and experimental geometry parameters and vibration frequencies for TT-COF.

Parameter		Exp. [18]	DFT
Bond length/Å	C39–S40	1.71	1.76
	B38–C39	1.46	1.53
	B34–O38	1.42	1.40
	C37–O34	1.32	1.38
	C37–C35	1.37	1.37
	C35–H56	1.00	1.08
Bond angles/°	C39–S40–C41	89.7	91.4
	C39–B38–O34	126.6	124.8
	B38–O34–C37	104.2	105.1
	O34–C37–C35	128.3	129.2
	C37–C35–H56	115.0	119.1
	C–S stretch	660	654
Vibration frequencies/cm ^{−1}	B–C stretch	1020	1014
	C–O stretch	1235	1283
	B–O stretch	1395	1318
	C=C for aromatics	1487	1487
	C=C for fused aromatics	1561	1564
	Emission spectrum/nm	475	450

3.2. Frontier molecular orbitals analysis and electronic configuration

Molecular orbitals analysis (MOs) is an intuitive way to get deep understandings of the nature of the excitation state related properties [30,31]. Owing to the Kasha's rule, the lowest excitation state of a given multiplicity is the most suitable for photon emission with a considerable quantum yield [32]. Therefore only the lowest excitation state S1 and the singlet state S0 were considered. In this context, the lowest unoccupied molecular orbital (LUMO) and the highest occupied molecular orbital (HOMO), as well as the electronic configuration for both TT-COF and TT-COF-HCHO complex, are described in detail. The electron density distribution on concerned molecules infers the possible effect on luminescence property. It is explicitly observed in Fig. 3a that LUMO electron density is mainly on thieno[3,2-*b*]thiophene boronic ester legend of TT-COF while for HOMO it is mostly distributed to HHTP moiety and also a small density portion is located on two of the attached boronic ester linkages. However, in the TT-COF-HCHO complex, the electron density distribution of LUMO is accumulated to the formaldehyde. On the contrary, the HOMO electron distribution seems further enriched on HHTP region same as the HOMO of TT-COF but alters both spin direction and color very clearly.

From frontier MOs evaluation, it can conclude that the non-covalent interactions significantly change the electron density distribution and may proceed the luminescence quenching accordingly. The luminescent property is delineated further, via electronic configuration from each atomic orbital. The LUMO electronic

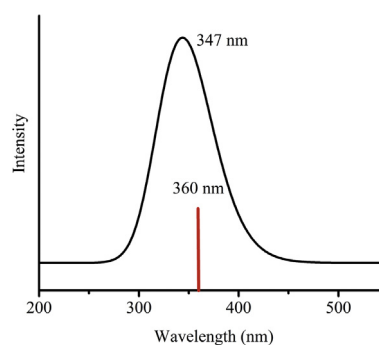


Fig. 2. Comparison of UV–Vis absorption. (Black line) representative computational. (Red line) for experimental (ref 18).

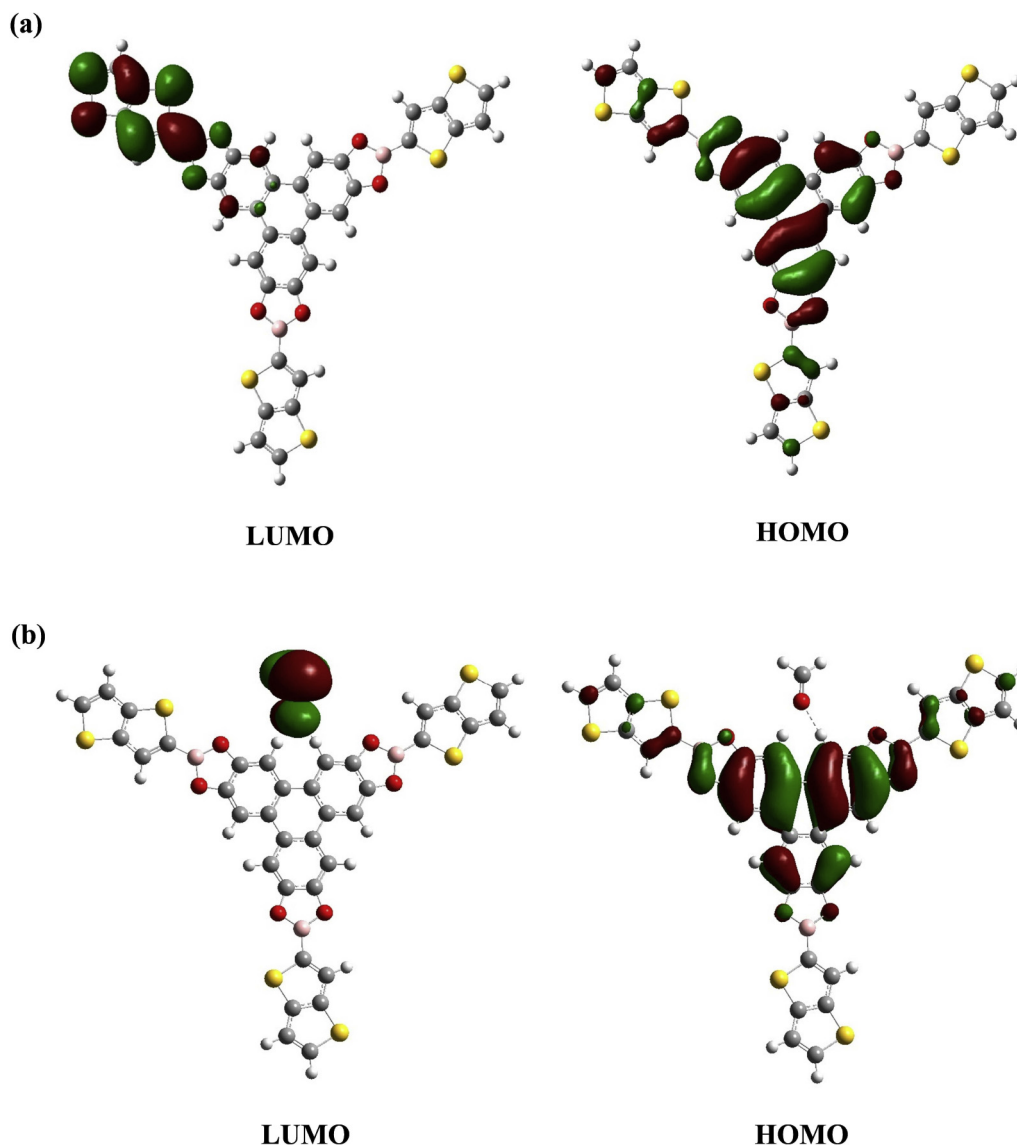


Fig. 3. The frontier molecular orbitals of (a) TT-COF and (b) TT-COF-HCHO complex.

configuration is comprised of P orbitals of C atoms (72.11%) and 9.79% O atoms respectively, whereas the C atoms (77.93%) P orbitals of HHTP and O atoms (8.66%) of boronic ester make the HOMO of TT-COF as mentioned in Fig. 4b. In the TT-COF-HCHO complex, the LUMO is made up of mainly P and S orbitals of C (62.08%), and P orbitals of oxygen (30.16%) while H, only (4.22%) atoms were of P orbitals respectively. Similarly, the HOMO consists of P orbitals, e.g., including C (77.16%) and O (7.24%) respectively. Thus, from the assessment of the MOs and electronic configuration, it is cleared that the encapsulated formaldehyde influences the electron density distribution effectively and enhances the contribution of hydrogen and oxygen atoms in robust intermolecular hydrogen bonded complex to change in luminescence consequentially.

3.3. Natural population analysis (NPA) analysis and electron density difference (EDD) map

In the noncovalent interacted complex, the charge transfer and polarisation can often occur. Therefore the electrons transfer and electron density polarisation are essential to investigate. In this context, NBO analysis can use to examine the weak interactions where electron distribution trend may be beneficial to describe the

transferring mechanism [33,34]. In this context, the net charges on desired atoms (H55, H56, and O70) are designated by NPA analysis for TT-COF, TT-COF-HCHO, and HCHO molecular systems, as shown in Table 2.

From Table 2, it is evident that the hydrogen bond formation brings a change in net charge on H55 and H56 for S₀ states of TT-COF-HCHO compared to free TT-COF unit is account for the strengthening of the hydrogen-bonded complex. In the S₀ hydrogen-bonded complex, the total charge on donor H55 changes from 0.248 to 0.253 of 0.005 charge while for H56 the net charge difference is 0.016 due to change from 0.236 to 0.252, respectively. Meanwhile, a further change occurs in S₁ hydrogen bond complex for hydrogen atoms H55, H56, like a 0.10 change in natural charge from 0.248 to 0.348 and 0.112 from 0.236 to 0.348 net charge respectively which describe the strengthening nature of hydrogen bonds.

Similarly, in Table 2, the net charge difference for O70 atom of the TT-COF-HCHO in the ground and excited states changes remarkably compared to free formaldehyde molecule. This charge change on O70 is −0.013 (from −0.519 to −0.532) while −0.372 change occurs (−0.519 to −0.891) for the S₁ state. Therefore, both results agree with the strengthening nature of the hydrogen bond may cause the charge transfer.

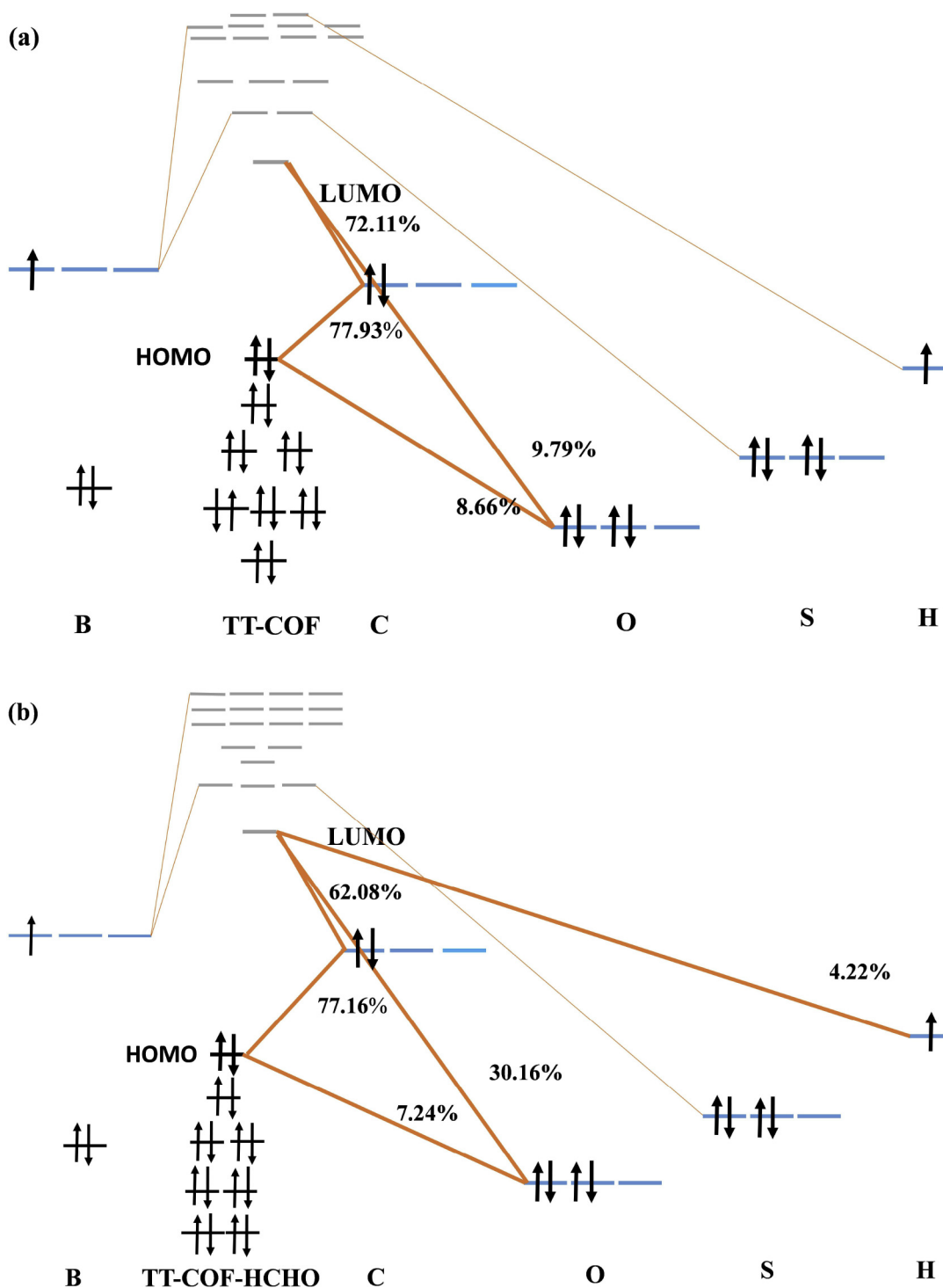


Fig. 4. The electronic configuration of (a) TT-COF and (b) TT-COF-HCHO complex.

Table 2

The NPA charge difference for selected atoms of TT-COF, TT-COF-HCHO, and HCHO molecule.

Atom	TT-COF	TT-COF-HCHO	HCHO
H55	0.248	0.253 (0.348)	—
H56	0.236	0.252 (0.348)	—
O70	—	−0.532 (−0.891)	−0.519

Another intuitive way to delineate the charge transfer via electron density variation for the weak interactions is the plotting EDD map using the Multiwfn software [27]. In Fig. 5, the EDD map is having positive (greenish) and negative (bluish) regions for TT-COF-HCHO complexes in the ground and excited states, respectively. In Fig. 5a, it is prominent that the positive charge located to hydrogen bonding region between hydrogen donor and hydrogen acceptor moieties. The excitation state bifurcated hydrogen bond indicates the noticeable accumulation of positive isosurface to its proximity Fig. 5b. However, the negative density region is distributed

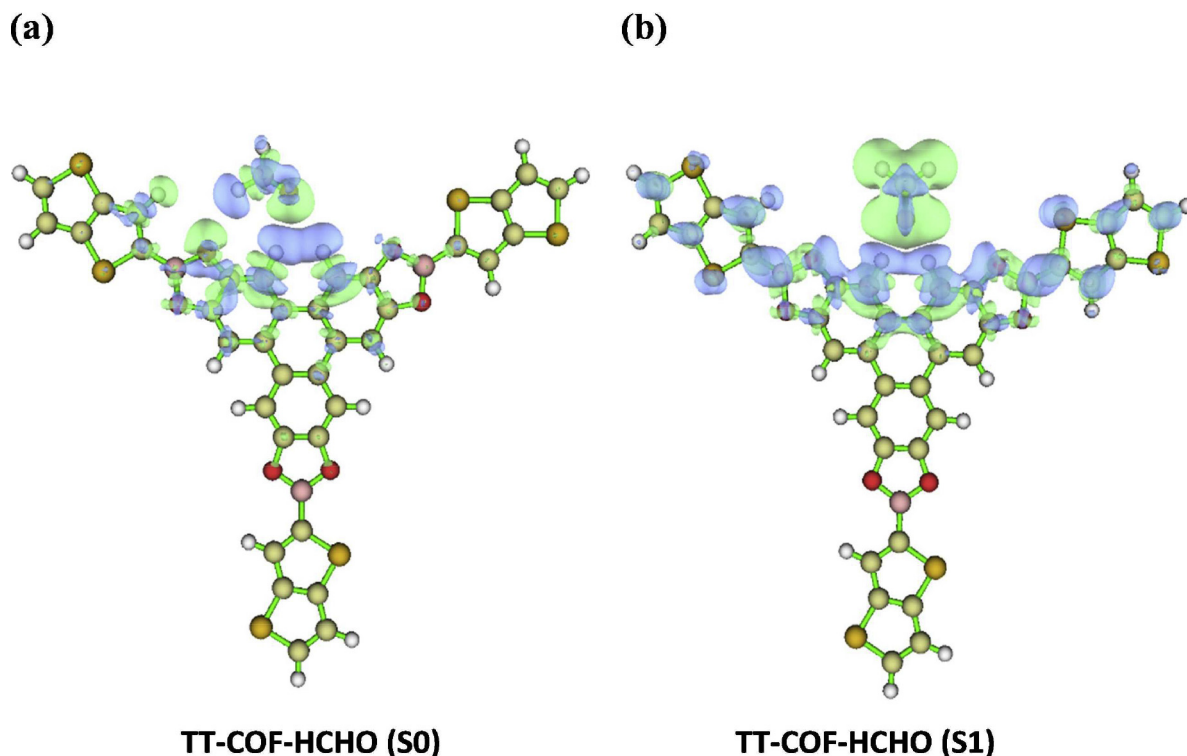


Fig. 5. The positive (greenish) and negative (bluish) regions in EDD map for (a) ground state and (b) excitation state.

uniformly to both TTBA legends. Moreover, thus, the EDD map can indicate the interaction and its effects explicitly; the strengthening hydrogen bond can give a basis for density variation in the interacted complex and the quenching also [35].

3.4. Electronic transition energies

Strong hydrogen bonds cause a redshift and affect the luminescence property [36]. Zhao et al. have summarised the electronically excited state hydrogen bonded complexes show a remarkable influence on transition energies [8,37,38]. According to Table 3, the first ten vertical transition energies for TT-COF and TT-COF-HCHO follow the Zhao et al. rule. The TT-COF-HCHO complex showed the redshifts and lower excitation energies compared to the isolated TT-COF, which further elucidate the strengthening behavior.

3.5. The behavior of the hydrogen bond in the electronically excited state

The hydrogen bonding dynamics in the excitation state can be elucidated by assessing the bond lengths, and binding energies. The given Table 4 lists the bond lengths for H55–O70 and H56–O70 of TT-

COF-HCHO. The H55–O70 bond distance is shortened by 0.8 Å from 2.67 Å to 1.87 Å. Similarly, the bond length of H56–O70 is also reduced by 0.52 Å, e.g., from 2.38 Å to 1.86 Å, respectively. The shortening bond distance for both H55–O70, and H56–O70 reveals the furcated hydrogen bond is explicitly enriched in the excitation state.

Another convenient way to monitor the hydrogen bonds strength is binding energy because the strong hydrogen bonds show the lower energy compared to weak hydrogen bonds [11]. In this context, it was observed that the binding energy in S0 was -7 kcal mol^{-1} while in the S1 state it was further decreased to $-21.53 \text{ kcal mol}^{-1}$. This noticeable change in binding energy also indicated the enhancement of the hydrogen bonds. Similarly, vibration frequency modes further, explain the nature of the hydrogen bonding dynamics. The strengthening of the hydrogen bonds causes redshifts in excitation state vibration modes in characteristic hydrogen donor and acceptor moieties [7,8]. The strengthening hydrogen bonding was estimated through the comparing of IR spectral changes from S0 to S1 states.

The prominent characteristic vibrational stretching modes, including symmetrical and antisymmetrical stretching, were thoroughly studied. The relevant bonds and their spectra are listed from left to right in Fig. 6. The frequency mode of C67=O70 remarkably decreased from 1812 cm^{-1} (S0) to 1529 cm^{-1} (S1) with 283 cm^{-1} of redshift, whereas the vibration mode appeared on 3236 cm^{-1} (S0) was the antisymmetric stretching mode of C3–H55 and C35–H56 bonds which apparently decreased to 3001 cm^{-1} (S1) state showed

Table 3
Electronic transition energies for TT-COF and TT-COF-HCHO.

Excitation states	TT-COF/eV	TT-COF-HCHO/eV
S1	3.57	3.43
S2	3.59	3.46
S3	3.63	3.52
S4	3.67	3.54
S5	3.65	3.58
S6	3.71	3.62
S7	3.71	3.66
S8	4.13	3.72
S9	4.16	3.98
S10	4.24	4.10

Table 4
The calculated hydrogen bonds and binding energy of TT-COF-HCHO complex in the S0 and S1 states.

Parameter		S0	S1
Bond length/Å	H55–O70	2.67	1.87
	H56–O70	2.38	1.86
Binding energy/kcal mol ⁻¹		-7.10	-21.53

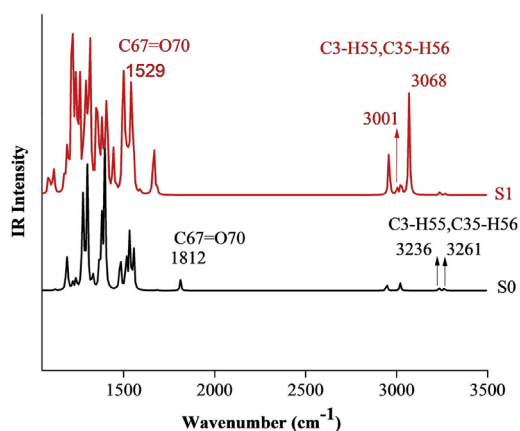


Fig. 6. Stretching vibration frequency of C67=O70 and C3-H55, C35-H56.

235 cm^{-1} redshift. Interestingly, this symmetric stretching frequency spectrum for both chemical bonds showed the same order from 3261 cm^{-1} (S0) to 3068 cm^{-1} (S1) by 193 cm^{-1} . Based on characteristic stretching frequencies of redshifts from the S0 to S1 state further manifested the strengthened hydrogen bonds.

3.6. Hydrogen bonding dynamics and radiationless processes

By a useful computational tool, the MOMAP, the luminescence and mobility properties of the organic materials can easily measure. This molecular property prediction package, MOMAP is more convenient to determine the optical spectra, fluorescence, phosphorescence, and radiative constants, IC, and ISC processes [29]. Additionally, this program satisfactorily evaluates the decaying mechanism with time-dependent perturbation and the Fermi Golden rule [39].

Herein, the calculated fluorescent rate constants for simulated TT-COF and TT-COF-HCHO complex are $1.16 \times 10^8 \text{ s}^{-1}$ and $1.45 \times 10^3 \text{ s}^{-1}$ respectively in Table 5. The lower radiative decay constant demonstrates the influence of the encapsulated formaldehyde on the luminescence of the TT-COF molecule, which concedes the strengthening nature of S1 hydrogen bonds. This program has successfully been used by Hao et al. to calculate the fluorescent rate constants of MOFs and COFs systems [13,40].

For further investigation of the quenching mechanism, we carried out the calculation for the S1-T1 energy gap because the radiationless process happens by involving the intersystem crossing, which may enhance the quenching [28,41]. The provided Table 5 denotes that the TT-COF-HCHO is having lower energy gap 0.32 eV relative to the isolated TT-COF molecule 1.00 eV. Thus, the hydrogen-bonded complex would show electronic coupling and thereby the maximum possibility of ISC. It is evident that the results of quenching constants, as well as the energy gap upon formaldehyde encapsulation, support the TT-COF is a promising chemosensor.

4. Conclusion

Keeping in view the understanding of the strengthening hydrogen bond results in the luminescence quenching, we

Table 5

The calculated fluorescent rate constant and S1-T1 energy gap difference for isolated TT-COF and TT-COF-HCHO complex.

	TT-COF	TT-COF-HCHO
Fluorescent rate constant/ s^{-1}	1.16×10^8	1.45×10^3
S1-T1 energy gap/eV	1.00	0.32

discovered the sensing potential of TT-COF for the indoor pollutant formaldehyde with employed DFT and TD-DFT methods as new dimensions in applications. From all over estimations; the bond lengths, electronic transition energies, binding energies, infrared spectra, UV-Vis and emission spectral shifts were pretty helpful to describe the strengthening nature of intermolecular hydrogen bonds.

From the frontier molecular orbitals, electronic configuration analysis, NPA analysis, and EDD map results confirmed apparently that the TT-COF luminescence mechanism became explicitly changed due to the formaldehyde induction. Furthermore, the performed fluorescent rate constants calculations also verified the quenching phenomenon for TT-COF-HCHO complex. The reason for the hydrogen bonding is due to the boronic ester functionality, which activates the C-H donor of the aromatic system and eventually causes significant hydrogen bonding. Results reveal that the TT-COF exhibits the remarkable sensitivity towards the formaldehyde pollutant. This intriguing and intuitive way can further use for sensing applications, particularly organic molecules, solvents, and various nitroaromatics and nitro explosives as well, to reveal their real-world uses.

Acknowledgments

We thank the National Natural Science Foundation of China (Grant Nos. 21606040 and 21677029), and the Fundamental Research Funds for the Central Universities (DUT18LK26).

References

- [1] E. Arunan, G.R. Desiraju, R.A. Klein, J. Sadlej, S. Scheiner, I. Alkorta, D.C. Clary, R.H. Crabtree, J.J. Dannenberg, P. Hobza, H.G. Kjaergaard, A.C. Legon, B. Mennucci, D.J. Nesbitt, Definition of the hydrogen bond (IUPAC Recommendations 2011), *Pure Appl. Chem.* 83 (2011) 1637–1641.
- [2] S. Bratoz, in: P.-O. Löwdin (Ed.), *Electronic Theories of Hydrogen Bonding*, Academic Press, 1967, pp. 209–237.
- [3] T. Chu, B. Liu, Establishing new mechanisms with triplet and singlet excited-state hydrogen bonding roles in photoinduced liquid dynamics, *Int. Rev. Phys. Chem.* 35 (2016) 187–208.
- [4] J.A. Gutierrez, R.D. Falcone, J.J. Silber, N.M. Correa, Role of the medium on the C343 inter/intramolecular hydrogen bond interactions. An absorption, emission, and 1H NMR investigation of C343 in benzene/n-heptane mixtures, *J. Phys. Chem. A* 114 (2010) 7326–7330.
- [5] V. Vetokhina, M. Kijak, G. Wiosna-Satyga, R.P. Thummel, J. Herbich, J. Waluk, On the origin of fluorescence quenching of pyridylindoles by hydroxylic solvents, *Photochem. Photobiol. Sci.* 9 (2010) 923–930.
- [6] M. Ramegowda, K.N. Ranjitha, T.N. Deepika, Exploring excited state properties of 7-hydroxy and 7-methoxy 4-methylcoumarin: a combined time-dependent density functional theory/effective fragment potential study, *New J. Chem.* 40 (2016) 2211–2219.
- [7] G.J. Zhao, K.L. Han, Early time hydrogen-bonding dynamics of photoexcited coumarin 102 in hydrogen-donating solvents: theoretical study, *J. Phys. Chem. A* 111 (2007) 2469–2474.
- [8] G.J. Zhao, K.L. Han, Hydrogen bonding in the electronic excited state, *Acc. Chem. Res.* 45 (2012) 404–413.
- [9] G.J. Zhao, K.L. Han, Role of intramolecular and intermolecular hydrogen bonding in both singlet and triplet excited states of aminofluorenones on internal conversion, intersystem crossing, and twisted intramolecular charge transfer, *J. Phys. Chem. A* 113 (2009) 14329–14335.
- [10] M. Conceição, D.A. Mateus, A.M. Da Silva, H.D. Burrows, UV-visible absorption spectra and luminescence of the pesticide fenarimol, *Spectrochim. Acta A Mol. Biomol. Spectrosc.* 53 (1997) 2679–2684.
- [11] Y. Yao, X. Song, J. Qiu, C. Hao, Interaction between formaldehyde and luminescent MOF [Zn(NH(2)bdca)(bix)]_n in the electronic excited state, *J. Phys. Chem. A* 118 (2014) 6191–6196.
- [12] Z. Zhao, X. Song, L. Liu, G. Li, S. Shah, C. Hao, A recognition mechanism study: luminescent metal-organic framework for the detection of nitro-explosives, *J. Mol. Graph. Model.* 80 (2018) 132–137.
- [13] Y. Wang, Z. Zhao, G. Li, Y. Yan, C. Hao, A 2D covalent organic framework as a sensor for detecting formaldehyde, *J. Mol. Model.* 24 (2018) 153.
- [14] C.S. Diercks, O.M. Yaghi, The atom, the molecule, and the covalent organic framework, *Science* 355 (2017) eaal1585.
- [15] S. Dalapati, E. Jin, M. Addicoat, T. Heine, D. Jiang, Highly emissive covalent organic frameworks, *J. Am. Chem. Soc.* 138 (2016) 5797–5800.
- [16] D. Kaleeswaran, P. Vishnoi, R. Murugavel, [3+3] imine and β -ketonamine tethered fluorescent covalent-organic frameworks for CO₂ uptake and nitroaromatic sensing, *J. Mater. Chem. C* 3 (2015) 7159–7171.

- [17] M. Ji, C. Hao, D. Wang, H. Li, J. Qiu, A time-dependent density functional theory study on the effect of electronic excited-state hydrogen bonding on luminescent MOFs, *Dalton Trans.* 42 (2013) 3464–3470.
- [18] M. Dogru, M. Handloser, F. Auras, T. Kunz, D. Medina, A. Hartschuh, P. Knochel, T. Bein, A photoconductive thienothiophene-based covalent organic framework showing charge transfer towards included fullerene, *Angew. Chem. Int. Ed.* 52 (2013) 2920–2924.
- [19] R. Golden, Identifying an indoor air exposure limit for formaldehyde considering both irritation and cancer hazards, *Crit. Rev. Toxicol.* 41 (2011) 672–721.
- [20] L. Zhang, L.E.B. Freeman, J. Nakamura, S.S. Hecht, J.J. Vandenberg, M.T. Smith, B.R. Sonawa, Formaldehyde and leukemia: epidemiology, potential mechanisms, and implications for risk assessment, *Environ. Mol. Mutagen.* 51 (2010) 181–191.
- [21] G.D. Nielsen, S.T. Larsen, P. Wolkoff, Re-evaluation of the WHO (2010) formaldehyde indoor air quality guideline for cancer risk assessment, *Arch. Toxicol.* 91 (2017) 35–61.
- [22] M.J. Frisch, G.W. Trucks, H.B. Schlegel, G.E. Scuseria, M.A. Robb, J.R. Cheeseman, G. Scalmani, V. Barone, B. Mennucci, G.A. Petersson, H. Nakatsuji, M. Caricato, X. Li, H.P. Hratchian, A.F. Izmaylov, J. Bloino, G. Zheng, J.L. Sonnenberg, M. Hada, M. Ehara, K. Toyota, R. Fukuda, J. Hasegawa, M. Ishida, T. Nakajima, Y. Honda, O. Kitao, H. Nakai, T. Vreven, J.A. Montgomery Jr., J.E. Peralta, F. Ogliaro, M. Bearpark, J.J. Heyd, E. Brothers, K.N. Kudin, V.N. Staroverov, R. Kobayashi, J. Normand, K. Raghavachari, A. Rendell, J.C. Burant, S.S. Iyengar, J. Tomasi, M. Cossi, N. Rega, J.M. Millam, M. Klene, J.E. Knox, J.B. Cross, V. Bakken, C. Adamo, J. Jaramillo, R. Gomperts, R.E. Stratmann, O. Yazyev, A.J. Austin, R. Cammi, C. Pomelli, J.W. Ochterski, R.L. Martin, K. Morokuma, V.G. Zakrzewski, G.A. Voth, P. Salvador, J.J. Dannenberg, S. Dapprich, A.D. Daniels, Ö. Farkas, J.B. Foresman, J.V. Ortiz, J. Cioslowski, D.J. Fox, Gaussian09 Revision D.01, Gaussian Inc., Wallingford CT, 2010.
- [23] A.D. Becke, Density-functional thermochemistry. III. The role of exact exchange, *J. Chem. Phys.* 98 (1993) 5648–5652.
- [24] G. Te Velde, F.M. Bickelhaupt, E.J. Baerends, C.F. Guerra, S.J.A. Van Gisbergen, J.G. Snijders, T. Ziegler, Chemistry with ADF, *J. Comput. Chem.* 22 (2001) 931–967.
- [25] C.F. Guerra, J.G. Snijders, G. te Velde, E.J. Baerends, Towards an order-N DFT method, *Theor. Chem. Accounts* 99 (1998) 391–403.
- [26] S. Simon, M. Duran, J.J. Dannenberg, How does basis set superposition error change the potential surfaces for hydrogen-bonded dimers? *J. Chem. Phys.* 105 (1996) 11024–11031.
- [27] T. Lu, F. Chen, Multiwfn: a multifunctional wavefunction analyzer, *J. Comput. Chem.* 33 (2012) 580–592.
- [28] M. Hussain, J. Zhao, W. Yang, F. Zhong, A. Karatay, H.G. Yaglioglu, E.A. Yildiz, M. Hayvali, Intersystem crossing and triplet excited state properties of thionated naphthalenediimide derivatives, *J. Lumin.* 192 (2017) 211–217.
- [29] Q. Peng, Y. Yi, Z. Shuai, J. Shao, Toward quantitative prediction of molecular fluorescence quantum efficiency: role of Duschinsky rotation, *J. Am. Chem. Soc.* 129 (2007) 9333–9339.
- [30] D. Wu, W. Mi, M. Ji, C. Hao, J. Qiu, The effect of furcated hydrogen bond and coordination bond on luminescent behavior of metal-organic framework [CuCN-EIN]: a TDDFT study, *Spectrochim. Acta Part A Mol. Biomol. Spectrosc.* 97 (2012) 589–593.
- [31] Y. Liu, Y. Yang, K. Jiang, D. Shi, J. Sun, Excited-state N-H...S hydrogen bond between indole and dimethyl sulfide: time-dependent density functional theory study, *Phys. Chem. Chem. Phys.* 13 (2011) 15299–15304.
- [32] M. Kasha, Characterization of electronic transitions in complex molecules, *Discuss. Faraday Soc.* (1950) 14–19.
- [33] Y. Zhang, Y. Duan, J. Liu, Time-dependent density functional theory study on the excited-state hydrogen-bonding characteristics of polyaniline in aqueous environment, *Spectrochim. Acta A Mol. Biomol. Spectrosc.* 171 (2017) 305–310.
- [34] A.E. Reed, R.B. Weinstock, Frank Weinhold, Natural population analysis, *J. Chem. Phys.* 83 (1985) 735–746.
- [35] A.E. Reed, L.A. Curtiss, F. Weinhold, Intermolecular interactions from a natural bond orbital, donor-acceptor viewpoint, *Chem. Rev.* 88 (1988) 899–926.
- [36] Y. Liu, J. Ding, D. Shi, J. Sun, Time-dependent density functional theory study on electronically excited states of coumarin 102 chromophore in aniline solvent: reconsideration of the electronic excited-state hydrogen-bonding dynamics, *J. Phys. Chem. A* 112 (2008) 6244–6248.
- [37] G.J. Zhao, K.L. Han, Effects of hydrogen bonding on tuning photochemistry: concerted hydrogen-bond strengthening and weakening, *ChemPhysChem* 9 (2008) 1842–1846.
- [38] G.J. Zhao, J.Y. Liu, L.C. Zhou, K.L. Han, Site-selective photoinduced electron transfer from alcoholic solvents to the chromophore facilitated by hydrogen bonding: a new fluorescence quenching mechanism, *J. Phys. Chem. B* 111 (2007) 8940–8945.
- [39] Q. Peng, D. Fan, R. Duan, Y. Yi, Y. Niu, D. Wang, Z. Shuai, Theoretical study of conversion and decay processes of excited triplet and singlet states in a thermally activated delayed fluorescence molecule, *J. Phys. Chem. C* 121 (2017) 13448–13456.
- [40] Z. Zhao, J. Hao, X. Song, S. Ren, C. Hao, A sensor for formaldehyde detection: luminescent metal-organic framework [Zn2(H2L)(2,2'-bpy)2(H2O)]n, *RSC Adv.* 5 (2015) 49752–49758.
- [41] Y. Dong, A. Iagatti, P. Foggi, J. Zhao, G. Mazzone, K. Xu, W. Ji, M. Di Donato, N. Russo, Bodipy-squaraine triads: preparation and study of the intramolecular energy transfer, charge separation and intersystem crossing, *Dyes Pigments* 147 (2017) 560–572.